Published in final edited form as:
Endocrinology. 2007 March ; 148(3): 1235–1245.

Posterior *Hox* Gene Expression and Differential Androgen Regulation in the Developing and Adult Rat Prostate Lobes

Liwei Huang, **Yongbing Pu**, **David Hepps**, **David Danielpour**, and **Gail S. Prins**
Department of Urology (L.H., Y.P., D.H., G.S.P.), University of Illinois at Chicago, Chicago, Illinois 60612; and the Ireland Cancer Center (D.D.), Case Western Reserve University, Cleveland, Ohio 44106

Abstract

Axis positioning and tissue determination during development involve coordinated expression of *Hox* genes throughout the body. The most posterior *Hox* gene clusters are involved in prostate organogenesis. In the present study, we characterized and compared the expression profiles of posterior (5′) *Hox* genes in the separate lobes of the adult rat prostate gland, the coagulating gland, seminal vesicles, and epididymis using quantitative real-time RT-PCR. These genes include *Hox*a9–11, *Hox*a13, *Hox*d13, and *Hox*b13. We identified a unique *Hox* code for each of these organs and propose that this contributes to the organ-specific and prostate lobe-specific identities in the adult rat. Using the ventral prostate (VP) as a model, we characterized the *Hox* genes expression patterns over time from birth through adulthood. Expression levels of the three *Hox*13 genes and *Hox*a10 were significantly higher in the adult VP compared with the neonatal developing VP suggesting an important role during adult homeostasis. In contrast, *Hox*a9 and *Hox*a11 levels declined after morphogenesis suggesting a specific developmental role. Overall, the *Hox*b13 gene exhibited the most striking temporal and organ-specific differences. Using *in situ* hybridization and immunohistochemistry, a distinct *Hox*b13 anterior-to-posterior expression gradient was observed with the highest expression levels in the VP luminal epithelial cells, moderate levels in the lateral prostate, and low expression in the dorsal prostate. An expression gradient was also observed along the ductal length in all three prostate lobes with strongest expression at the distal tips and limited expression in the proximal ducts. After infection with a lentivirus expressing the *Hox*b13 gene, NRP-152 cells cultured under nondifferentiating conditions exhibited robust cytokeratin 8 immunostain indicating that *Hox*b13 expression drives luminal cell differentiation in the rat epithelium. Androgen regulation of prostatic *Hox* gene expression was examined during development *in vitro* and after castration in the adult rat. In the neonatal VP, all six *Hox* genes were significantly up-regulated by androgens, whereas none of the genes were affected by testosterone in the lateral prostate. In the adult rat, castration resulted in up-regulation of *Hox*a9 and *Hox*a13 in the VP and down-regulation of *Hox*b13 in the dorsal prostate and lateral prostate. Taken together, we conclude that the prostatic *Hox* genes reach a destined expression level at specific developmental time points in the prostate gland and possess differential androgenic regulation in a temporal and lobe-specific manner. We suggest that this timely *Hox* code participates in determining lobe-specific prostatic identity and cellular differentiation.

Axis positioning and tissue determination during development involve the coordinated expression, function, and interplay of a superfamily of homeobox genes. These master regulatory genes encode transcription factors that contain a highly conserved polypeptide segment, designated the homeodomain, which binds to regulatory regions of target genes (1).

Address all correspondence and requests for reprints to: Gail S. Prins, Department of Urology, MC 955, University of Illinois at Chicago, 820 South Wood Street, Chicago, Illinois 60612. E-mail: gprins@uic.edu.

Disclosure Statement: The authors have nothing to declare.

The most extensively studied members of this superfamily are the *Hox* genes, which determine patterning and tissue specification in body regions from *Drosophila* to humans. In mammals, gene duplication has led to four *Hox* clusters (a, b, c, and d) on separate chromosomes encoding a total of 39 genes (2). Similar genes in the separate clusters are considered paralogs and frequently, although not always, have overlapping functions. Expression of the genes, from the 3′ to the 5′ end of each cluster, follows a pattern of spatial and temporal colinearity during embryogenesis. In general, the 3′ genes designate anterior regions, whereas the 5′ or posterior genes encode posterior regions. A generalized model for regional tissue specification exploits nested, partially overlapping expression of several genes in a *Hox* cluster to determine segment or tissue identity.

The anterior-to-posterior axis of the rodent male reproductive tract consists of the epididymis, vas deferens, seminal vesicles, coagulating gland, dorsal prostate, lateral prostate, ventral prostate gland, and bulbourethral glands. Although the epididymis, vas deferens, and seminal vesicle are derived from the mesodermal Wolffian ducts, the prostate and bulbourethral glands are of endodermal urogenital sinus (UGS) origin. The coagulating gland is a unique hybrid of UGS epithelium and Wolffian duct mesenchyme. Because the prostate gland is one of the most posterior organs in vertebrates, it was not unexpected that the *Hox*13 genes, the most posterior of the *Hox* clusters, are involved in prostate organogenesis (3). Individual studies with murine prostates have shown that *Hox*a13 is highly expressed in the mesenchyme with lower epithelial expression (4), whereas *Hox*d13 is localized to both epithelium and mesenchyme in the fetal and neonatal prostate (5,6). Notably, both studies found a rapid decrease in expression during morphogenesis with low adult expression levels. In contrast, *Hox*b13 localized exclusively to epithelial cells in the murine prostate and expression levels increased postnatally (7–9). To date, *Hox*c13 has not been found in the prostate gland (10). Studies using null mutant mice for specific *Hox*13 paralogs have shown essential roles for these genes during prostate development. *Hox*d13$^{-/-}$ mice exhibit reductions in size and ductal branching of all prostate lobes indicating a specific role in those developmental growth events (11). Although *Hox*a13$^{-/-}$ mice are embryonic lethal, compound *Hox*a13$^{+/-}$/*Hox*d13$^{-/-}$ mutants show severe prostatic growth defects (3) implying an essential role for *Hox*a13 in prostate growth. This is supported by heterozygous *hypodactyly* mice with a *Hox*a13 exon 1 deletion, which show hypomorphic prostate lobes (4). Targeted deletion of *Hox*b13 resulted in aberrant epithelial differentiation and loss of secretory capacity in the mouse ventral prostate suggesting an important role in epithelial cell differentiation (9). One additional report showed low expression of *Hox*a10 in the murine prostate during fetal life but no expression postnatally, suggesting that more anteriorly expressed *Hox* genes play a role during prostate development (12). However, no prostatic phenotype was found in Hoxa10$^{-/-}$ mice.

Although studies on *HOX* gene expression in the human prostate are limited, several reports on human prostate tissue and cell lines have shown the expression of *HOX*13 paralogs as well as several anterior *HOX* genes (10,13–15). Although clear functions have not been ascribed to specific *HOX* genes in the adult prostate, research on human prostate cancer has identified the potential involvement of *HOX* gene dysregulation in human prostate cancers (14,16–18). Based on these reports, it has been suggested that normal *HOX* expression is necessary for homeostasis of the gland.

Although autoregulation and crossregulation between *Hox* genes has been demonstrated (19), the factors that tightly regulate tissue-specific and temporal expression of *Hox* genes are not well understood. There is clear evidence, however, that *Hox* gene expression is regulated by steroids in specific structures (20). Most notably, retinoids regulate the expression of *Hox* genes during development with a particular emphasis on anterior *Hox* genes and a declining regulatory capacity for the posterior *Hox* genes (20,21). Control of posterior *Hox* genes in the female reproductive tract has been found to be dynamically regulated by estrogens and

progesterone and, under pathological conditions, by testosterone (20,22,23). Although *Hox*b13 expression in the adult mouse prostate (7) and human prostate cancer cells (13) was found to be androgen-independent, hormonal regulation of other prostatic *Hox* genes has not been examined.

The rat prostate gland has been a traditional model for prostate research for several decades. Although direct analogies to the human prostate are not possible, the rat prostate gland is larger and more complex than the mouse prostate, making it a superior model for comparative studies (24). The rat prostate gland consists of three distinct prostate lobes, the dorsal (DP), lateral (LP), and ventral lobes (VP), with unique secretions (25–27) that serve as excellent models for tissue heterogeneity. All three lobes exhibit extensive and intricate branching patterns compared with the poorly branched murine prostate. Furthermore, although the LP is rudimentary in the mouse (24), the rat LP is complex with distinctive LP1 and LP2 branched structures (27). This is particularly significant because the LP is considered to most resemble the human prostate embryologically and histologically (28). The molecular basis for regional heterogeneity in the rat as well as human prostate is not well understood. Interestingly, the expression of *Hox* genes in the rat prostate gland has not been previously reported.

In the present study, we sought to characterize and compare the posterior (5′) *Hox* gene expression profiles in the separate adult rat prostate lobes with the goal of uncovering a molecular basis for prostate lobe-specific identity. Because the *Hox*13 paralogs have been identified as critical for prostate structures, we examined expression of all *Hox*13 genes using quantitative methods that permit direct comparisons of gene expression levels. In addition, prostatic expression of the more anterior *Hox*a9, *Hox*a10, and *Hox*a11 genes was measured because they play an important role in anterior structures of the male reproductive tract (29). We also examined expression of these *Hox* genes in the coagulating gland, seminal vesicles, and epididymis to determine expression boundaries and similarities with adjacent anterior structures. *Hox* gene expression was further profiled from birth through adulthood in the rat VP to track changes in expression levels over development. Because an increasing gradient of *Hox*b13 expression along the anterior to posterior reproductive tract axis was the most notable difference between tissues, its localization and function were examined in further detail. Finally, because prostate development and adult homeostasis is dependent on androgens, regulation of prostatic *Hox* gene expression by testosterone was evaluated during early development and in the mature gland. Our results identify unique *Hox* codes for each prostate lobe as well as regional and temporal differences in androgenic regulation that may explain, in part, regional tissue specification within the rat prostate gland.

Materials and Methods

Animals

All rats were handled in accordance with the principles and procedures of the Guiding Principles for the Care and Use of Animal Research and the experiments were approved by the Institutional Animal Care Utilization Committee. Timed pregnant female Sprague-Dawley rats were purchased from Zivic-Miller (Pittsburgh, PA), housed individually in a temperature (21 C) and light (14 h light, 10 h dark)-controlled room and given standard Purina rat chow (Ralston-Purina, St. Louis, MO) and water *ad libitum*. They were monitored daily for delivery of pups and the day of birth was designated as d 0. At d 23, male rats were weaned and housed as described previously with three animals per cage. For adult *Hox* gene studies, rats were killed on d 90 and the separate VP, DP, and LP lobes, the coagulating gland, seminal vesicles (fluid expressed), and entire epididymis were removed and snap-frozen in liquid nitrogen. For developmental studies, male rats were killed on d 1, 3, 6, 10, 30, or 90 of life (n = 3–10 for each time point) and the VP was removed and frozen in liquid nitrogen. For adult studies with testosterone withdrawal, d 90 rats were castrated through the scrotal route under ketamine/

xylazine anesthesia (50 mg/kg Ketaset; Brisol Laboratories, Syracuse, NY; and 10 mg/kg Rompum; Mobay Corp., Shawnee, KS). Intact and 48-h castrated rats (n = 6 for each group) were killed by decapitation; prostate lobes were dissected and placed on ice before RNA extraction.

Prostate organ culture

For developmental regulation of *Hox* gene expression by androgens, short-term organ culture experiments were performed. VPs and LPs were isolated on the day of birth by manual dissection under a microscope and immediately cultured on Millicell-CM filters (Millipore Corp., Bedford, MA) floating in 2 ml nutrient medium in BD Falcon six-well plates (BD Biosciences, San Jose, CA). The basic organ culture medium (BOCM) consisted of DMEM/F-12 (Invitrogen/GIBCO, Carlsbad, CA), 50μg/ml gentamicin, and 1× insulin-transferrin-selenium (Invitrogen). One VP and LP lobe from each animal (n = 8) was individually cultured for 18 h in BOCM with OH-flutamide (Schering Corp., Bloomfield, NJ) to block endogenous androgen action while the contralateral lobe from each animal was individually cultured in BOCM with 10 nM testosterone (Sigma-Aldrich, St. Louis, MO). The VPs and LPs were cultured in a humidified 5% CO_2 incubator for 18 h, which allowed sufficient time for gene expression responses to androgens while avoiding marked shifts in the mesenchymal/epithelial ratio observed with growth during extended culture. Culture was terminated at 18 h and RNA was immediately isolated from the individual prostate lobes for subsequent use in real-time RT-PCR. The assay was repeated 10 times with separate rats used for each assay.

Quantitative real-time RT-PCR

Two procedures were used for RNA extraction and RT depending on tissue volume. A standard assay for all adult tissues and for VPs on d 6 through 90 involved RNA extraction with Trizol (Invitrogen), DNase I digestion (Roche, Indianapolis, IN), and RT with avian myeloblastosis virus at 42 C for 60 min using the RT System (Promega, Madison, WI). For smaller tissues (all postnatal d 1, three tissues), RNeasy Mini Kit (Qiagen, Valencia, CA) was used for RNA extraction and On-Column DNase I digestion and RT with MMLV at 37 C for 60 min using First Strand cDNA Synthesis Kit (Fermentas Inc., Hanover, MD). Random primers were used for RT.

Real-time PCR was performed in duplex with Platinum qPCR Supermixture-UDG (Invitrogen) using an iCycler (Bio-Rad, Hercules, CA) as previously described (30). Reaction conditions were optimized for each gene and the cycle conditions were 95 C for 3 min and 40 cycles of 95 C for 15 sec and 60 C for 30 sec. The exon-spanning primers and dual-labeled probes are listed in Table 1. For dual-labeled probes, 5′ reporters were FAM for *Hox*a9, *Hox*a11, *Hox*b13, and *Hox*d13 and Hex for *Rpl*19. The 3′ quencher was a black hole quencher. SYBR green assay was performed for *Hox*a10 and *Hox*a13 and melting curve analysis confirmed the product specificity. A PCR product of 300 to 600 bp for each gene was cloned into PCRII plasmid (Invitrogen) and the identity of the inserts was confirmed by DNA sequencing. The plasmids were used for standard curves in each reaction to directly quantitate target DNA levels. Ribosomal protein L19 (*Rpl*19) was quantitated and served as an internal reference for normalization. Optical data obtained by real-time PCR was analyzed with the manufacturer's software (iCycler Optical System Interface version 3.1). Each assay was repeated three to 11 times using different tissues.

In situ hybridization

The rat *Hox*b13 RNA probe was prepared by cloning a 374 bp *Hox*b13 PCR product into PCRII plasmid, which was confirmed by sequencing. To synthesize an antisense or sense RNA probe, plasmid DNA was linearized with *Hin*dIII or *Xho*I, respectively, and transcribed with T7 or SP6 RNA polymerase, respectively, using the DIG RNA Labeling Mix (Roche). Paraffin-

embedded prostate complexes from d 10 and 30 rats and individual lobes from d 90 rats were sectioned (4 μM), deparaffinized in xylene, rehydrated with alcohol, and fixed in 4% paraformaldehyde for 10 min at room temperature. Tissue sections were digested with proteinase K (10 μg/ml, 37 C for 30 min) and acetylated with acetic anhydride. After prehybridization, each slide was hybridized for 16 to 20 h at 57 C in buffer containing 50% deionidized formamide, 10% dextran sulfate, 1× Denhardt's solution, 10 mM Tris-HCl (pH 7.6), 600 mM NaCl, 0.25% sodium dodecyl sulfate, 1 mM EDTA, 2 mg/ml transfer RNA, 100 μg/ml sheared salmon DNA, and 2 μg/ml denatured digoxygenin-11-UTP-labeled cRNA probe. The slides were rinsed in 5 × SSC at 57 C for 10 min, washed twice in 50% formamide in 2× SSC at 57 C for 30 min, and twice in 0.2× SSC for 30 min at 57 C. After blocking with 1% blocking reagent, the slides were incubated with sheep anti-DIG fab′ antibody (1:1000; Roche) for 2 h at 37 C. After color development, the slides were dehydrated with alcohol, cleared with xylene, and cover-slipped with Permount (Fisher Scientific, Itasca, NY).

NRP-152 cell culture and lentiviral-Hoxb13 infection

The NRP-152 cell line was used to examine *Hox*b13 function *in vitro*. NRP-152 cells originated from a Wistar-Lobund rat dorsolateral prostate, which spontaneously immortalized in culture (31). These androgen-responsive, nontumorigenic cells exhibit basal epithelial cell characteristics when cultured under normal growth conditions (high serum) and transdifferentiate to a luminal epithelial phenotype under growth-restrictive conditions (low serum) or with the addition of TGFβ1 (32). The NRP-152 cells used in this study (between passages 20 and 30) were grown in a 5% CO_2 atmosphere at 37 C under normal growth conditions in GM2 (DMEM/F12, 5% fetal bovine serum, 0.1 μM dexamethasone, 5 μg/ml insulin, 20 μg/ml epidermal growth factor, 10 ng/ml cholera toxin) as described (31). Cultures were maintained at less than 70% confluence.

The plasmids for constructing a lentivirus, pHR′-CMV-EGFP, pCM-VDR8.2, and pMD.G, were kindly provided by Dr. Paul Rennie at University of British Columbia, Canada. The EGFP gene was removed from the pHR′-CMV-EGFP plasmid at BamH1-Kpn1. The protein-coding region of the human *HOX*b13 gene in pPROEXHTa plasmid (generously supplied by Dr. Charles Bieberich, University of Maryland) was cut by *Bam*H1 and *Kpn*1 and inserted into the complementary site of pHR′-CMV-plasmid (without EGFP) to create a pHR′-CMV-*Hox*b13 plasmid. The orientation of the construction was checked by endorestriction enzyme digestion. The method for lentiviral preparation and viral titer estimation were prepared as described (33) with minor modifications. Briefly, 1.5×10^6 293T cells were seeded onto 10-cm plates and cotransfected the next day by lipofectamine 2000 (Invitrogen) with 10 mg of pHR′-CMV-*Hox*b13 or pHR′-CMV-EGFP, 10 mg of pCMVDR8.2, and 5 mg of pMD.G for 12 to 16 h followed by a change in medium. The vector-conditioned medium was collected 72 h after transfection and the aliquots were stored at −70 C for future use.

NRP-152 cells were plated in either six-well plates or two-chamber slides in GM2 medium for 24 h before infection with lentivirus. Several dilutions of virus at different multiplicity of infection containing 8 μg/ml polybrene (Sigma) were added to each well of cultured cells. The virus-containing medium was removed 20 h after infection and replaced with fresh GM2 medium. Seventy-two hours after infection, cells grown on six-well plates were trypsinized and processed for RNA isolation, whereas cells grown in two-chamber slides were washed with PBS and fixed for immunofluorescent staining.

To confirm infection of NRP-152 cells with *Hox*b13-lentivirus, total RNA was extracted with RNeasy Kit (Qiagen, Valencia, CA) followed by RT with iScript cDNA Synthesis Kit (Bio-Rad). The resulting cDNA were subjected to end-point PCR. The length of the expected product and sequences of the primers set used were as follows: *Hox*b13; 256 bp, 5′-TTCCCGTGGACAGTTACCAG-3′, and 5′-TTGCGCCTCTTGTCCTTAGT-3′; *Rpl*19; 585

bp, 5′-AGGCTACAGAAGAGGCTTGC-3′, and 5′-GACGCTTCATTTCTTGGTCTC-3′. PCRs were performed under the following conditions: 95 C for 2 min followed by 35 cycles of 95 C for 1 min, 57 C for 1 min, and 72 C for 2 min; and 72 C for 5 min. PCR products were analyzed by DNA electrophoresis in 1.5% agarose gel in 1× TAE buffer. Protein expression of *Hox*b13 was confirmed by immunocytochemistry.

Immunocytochemistry and immunohistochemistry

NRP-152 were fixed in 4% paraformaldehyde/0.2% picric acid for 10 min and permeabilized with 0.1% Triton X-100 in PBS for 20 min. The cells were blocked with Superblock (Pierce, Rockford, IL) for 30 min and incubated overnight at 4 C with mouse antihuman cytokeratin (CK) 8 antibody (Jackson ImmunoResearch Laboratories, West Grove, PA) and rabbit anti-human *Hox*b13 antibody (kindly supplied by Dr. Bieberich) at a 1:100 dilution. Cells were next incubated with Cy3-conjugated antimouse and fluorescein isothiocyanate-conjugated antirabbit secondary antibody (Jackson ImmunoResearch) at 37 C for 1 h and were washed with PBS/gelatin and deionized water. Coverslips were mounted with Vectashield containing DAPI (Vector Laboratories, Burlingame, CA) to visualize nuclei. Multichannel photographs of the fluorochrome-labeled slides were taken using a Carl Zeiss Axioskop and Zeiss black and white Axiocam digital camera (Carl Zeiss, New York, NY) with color rendition made in Adobe Photoshop.

*Hox*b13 protein was localized in VP lobes taken from d 6, 10, and 30 rats using immunohistochemistry as previously described (34). In brief, frozen prostatic complexes were sectioned at 6 μm on Superfrost Plus slides (Fisher Scientific) and fixed in 2% paraformaldehyde. After treating with Superblock, sections were incubated overnight at 4 C with rabbit antihuman *Hox*b13 antibody (1:2500). The primary antibody was reacted with biotinylated goat anti-rabbit IgG secondary antibody (Vector Laboratories) and detected with an avidin-biotin peroxidase kit (ABC-Elite; Vector Laboratories) using diaminobenzidine tetrachloride as a chromagen. The sections were counterstained with Gill's no. 3 hematoxylin (1:4). For controls, 1 μg/ml normal rabbit IgG (Vector Laboratories) was substituted for primary antibody on separate sections to determine nonspecific binding.

Statistics

Real-time RT-PCR results were analyzed by two-tailed Student's *t* test for two group comparisons or ANOVA for multiple group comparisons followed by Bonferroni *post hoc* tests (Instat version 3.01; GraphPad Software, Inc., San Diego, CA). Results are expressed as mean ± SEM and $P < 0.05$ or less was accepted as significant.

Results

Expression of Hox genes in adult male accessory sex glands: organ-specific and prostate lobe-specific Hox codes

Real-time RT-PCR was used to quantitate *Hox*a9–11, *Hox*a13, *Hox*d13, and *Hox*b13 expression in d 90 intact rat epididymis, seminal vesicle, coagulating gland, DP, LP, and VP prostate lobes. The relative expression levels for each *Hox* gene in the different organs are shown in Fig. 1 (*left panel*). The *Hox*13 genes were most abundant in the prostate lobes and coagulating gland with decreased expression in the more anterior seminal vesicle and no expression in the epididymis. Most prominently, *Hox*b13 was entirely restricted to the prostate with a striking decline from the posterior VP to the anterior coagulating gland. This supports the concept that *Hox*b13 is involved in posterior prostate identity. In contrast to the *Hox*13 genes, the *Hox*a9–11 genes were expressed at one to two lower orders of magnitude in the male accessory sex glands. Noteworthy is the observation that *Hox*a9 expression was higher in the posterior prostate lobes, particularly the LP, and lowest in the more anterior epididymis.

Additionally, *Hox*a10 expression was similar in the epididymis, coagulating glands, and the dorsolateral prostate while lower in the seminal vesicles and VP. In contrast, *Hox*a11 expression was similar across all accessory sex glands.

When comparing the *Hox* gene expression levels in the individual accessory sex glands, a unique *Hox* "code" was observed for each organ (Fig. 1, *right panel*). The most anterior structure, the Wolffian duct (mesodermal) -derived epididymis, was characterized by high expression of *Hox*a10 and absence of all *Hox*13 genes. Moving posteriorly, the Wolffian-derived seminal vesicle had lower *Hox*a10 expression, moderate *Hox*a13, and strong *Hox*d13 expression but no *Hox*b13. The coagulating gland, derived embryonically from both the Wolffian duct and endodermal UGS, had a *Hox* code similar to the seminal vesicle with the addition of detectable but low levels of *Hox*b13. The prostate lobes, derived entirely from the UGS, possessed *Hox* codes characterized by high levels of all *Hox*13 genes. Nonetheless, each lobe had distinct profiles with *Hox*a13 and *Hox*d13 expression declining and *Hox*b13 expression increasing in the posterior direction. Thus, the DP had higher *Hox*a13 and *Hox*d13 levels and lower epithelial *Hox*b13 levels than the LP and VP. Although the LP and VP possessed similar *Hox*a13 and *Hox*d13 levels, *Hox*a9–11 expression was higher in the LP, whereas *Hox*b13 expression was higher in the VP. The VP was unique with the highest *Hox*b13 expression and the lowest levels of *Hox*a9–11 among the three prostate lobes.

Hox gene expression patterns in the developing rat prostate

The ontogeny of *Hox* gene expression in the prostate gland was examined using the VP as a model as a result of its larger size and unique *Hox* code. As shown in Fig. 2, *Hox*a9 and *Hox*a11 expression was highest at d 1 to 3 of life and steadily declined thereafter to nadirs at d 10 and 30, respectively, where they remained through adulthood. In contrast, *Hox*a10 and all *Hox*13 genes were expressed at low levels at birth and increased after morphogenesis, reaching high expression levels in adulthood. At that time, the *Hox*13 genes had over 10-fold higher expression levels than the *Hox*a9–11 genes. Among the three *Hox*13 gene paralogs, the increase of *Hox*a13 and *Hox*d13 over development was two- to threefold, whereas *Hox*b13 expression increased over 200-fold by adulthood. These differences may be in part a reflection of their differential localization because *Hox*a13 and *Hox*d13 are expressed in the stroma (4,5), which increases minimally in total mass as the organ grows, whereas *Hox*b13 is expressed exclusively in epithelial cells, which show a massive increase in number with development and growth.

Hoxb13 expression and localization in the separate prostate lobes

Because expression of the *Hox*b13 gene exhibited the most striking temporal and organ-specific differences, its localization and function were examined in further detail. *In situ* hybridization was performed to characterize its spatial expression pattern over time in the individual prostate lobes. Although detected at low levels by RT-PCR as early as d 3 of life, *Hox*b13 was first detectable in epithelial cells by *in situ* hybridization at d 10 with similar staining intensity within the VP, LP, and DP lobes (Fig. 3, A–C). By d 30 when luminal epithelial cells were fully differentiated, a distinct expression gradient was observed with the highest *Hox*b13 expression in VP luminal epithelial cells, moderate levels in the LP, and low expression in the DP (Fig. 3, D–H). Furthermore, an expression gradient was observed along the ductal length in all three lobes with strongest expression at the distal tips and limited expression in the proximal ducts (Fig. 3I). Immunohistochemistry confirmed a similar temporal pattern with *Hox*b13 protein localized to epithelial cell nuclei by d 10 and peak levels at d 30 of life (Fig. 3, J–L).

Hoxb13 expression drives differentiation of prostatic epithelial cells

The physiological function of *Hox*b13 in controlling luminal differentiation of prostate epithelium was explored in the rat prostate epithelial cell line, NRP-152, which has stem cell

behavior *in vitro* (32) and has the unique ability to develop normal prostatic organoids in tissue recombinants with UGM placed under the renal capsule (35). When grown in 5% serum, NRP-152 rat prostate epithelial cells possess a basal cell phenotype with localization of p63 and CK5/15 but lack CK8 and *Hox*b13 gene expression by RT-PCR (Fig. 4A). To directly assess whether *Hox*b13 plays a role in normal rat prostate epithelial cell differentiation, NRP-152 cells were infected with a lentivirus expressing the *Hox*b13 gene. Confirmation of *Hox*b13 infection was determined by end-point RT-PCR, which showed a strong *Hox*b13 band in pHR′-CMV-*Hox*b13-infected cells but no *Hox*b13 DNA in control cells infected with pHR ′-CMV-EGFP (Fig. 4C). Additionally, *Hox*b13 protein was localized to nuclei of pHR′-CMV-*Hox*b13-infected cells, whereas cells infected with the control pHR′-CMV-EGFP vector were negative for *Hox*b13 protein (Fig. 4B). After 3 d of culture in nondifferentiating medium (GM2 with 5% serum), *Hox*b13-infected and control cells were examined for evidence of luminal epithelial differentiation using CK8 as a luminal cell marker. Although control cells showed minimal staining for CK8, NRP-152 cells with forced expression of *Hox*b13 protein exhibited robust CK8 immunostaining (Fig. 5, A and B). Because infection efficiency varied between 20% and 60% of cells, *Hox*b13 protein and CK8 were colocalized in the pHR′-CMV-*Hox*b13 infected NRP-152 cells. As shown in Fig. 5, C and D, cells with nuclear *Hox*b13 protein also expressed cytoplasmic CK8, whereas noninfected cells were CK8-negative. These data support the premise that *Hox*b13 expression drives luminal cell differentiation in the normal rat prostate epithelium.

Differential androgen regulation of prostatic Hox genes in the developing and adult prostate lobes

Regulation of *Hox* gene expression by androgens in the developing rat prostate was examined in short-term VP and LP organ cultures in the absence of androgen action (BOCM plus OH-flutamide) and the presence of 10 nM testosterone. Under these conditions, all of the *Hox* genes examined were significantly up-regulated by androgens in the VP (Fig. 6A). Of note, the *Hox*a9 and *Hox*a11 genes showed the greatest expression increase by androgens, whereas the *Hox*13 paralogs were only modestly increased after 18 h exposure to testosterone. In contrast, none of the examined *Hox* genes were affected by testosterone in the developing LP lobes (Fig. 6B).

Androgen regulation of the adult prostate *Hox* genes was examined by androgen removal by castration of rats at d 90. Because androgen levels reach a nadir within 24 h after castration (36), although marked protein, RNA, and DNA loss does not occur until after 48 h (37), prostate *Hox* gene expression was examined at 48 h after castration to avoid interpretation difficulties associated with involution. Importantly, lobe-specific affects of hormone withdrawal were observed. In contrast to developmental up-regulation by androgens, only *Hox*a9 and *Hox*a13 were affected by androgen removal in the VP (Fig. 7A). Interestingly, expression of both genes was increased by castration indicating that androgens down-regulate expression of these genes in the adult prostate. In the DP and LP, only *Hox*b13 expression was affected by castration and because it was significantly reduced, this indicates that *Hox*b13 is positively regulated by androgens in those lobes (Fig. 7, B and C). Although there was a trend for *Hox*b13 reduction after castration in the VP, it was not significant.

Discussion

Hox genes play an important role during tissue specification in the body where they regulate cell proliferation and fate determination. Additionally, *Hox* genes are believed to be essential in the maintenance of homeostatis in adult structures. In the present study, we have identified specific and unique *Hox* codes for each of the prostate lobes and other accessory sex glands that contribute to the organ-specific and lobe-specific identities in the rat. Overall, this fits the

paradigm that *Hox* gene combinations give rise to unique structures throughout the body. As previously demonstrated for the mouse (3–5,7), the *Hox*13 paralogs are the predominantly expressed *Hox* genes in the rat prostate gland, although various combinations and levels of anterior *Hox* genes are also expressed. Similar findings in a human screen of *HOX* genes in adult organs noted expression of many anterior *HOX* genes in posterior structures, including the prostate, albeit at lower levels in the prostate than the *Hox*13 genes (10). It is notable in the present study that expression of the more anterior *Hox*a9 gene peaked in the LP and was significantly lower in the more anterior epididymis, which suggests a more prominent role for *Hox*a9 in lateral lobe development. It is also noteworthy that a strict colinear anterior-to-posterior gradient was not observed for several of the *Hox* genes. In particular, *Hox*a10 initially declined from the epididymis to the posterior seminal vesicle but then rose in the more posterior prostate lobes, whereas *Hox*a11 gene expression did not vary along the reproductive tract axis. Another important observation in the present study was that the dynamic expression of several *Hox* genes, including all *Hox*13 genes, increased after completion of development suggesting perhaps a more important role in maintaining the adult phenotype compared with a developmental role.

Although similar *Hox* genes are expressed in the rat and mouse prostate, their spatial and temporal patterns differed markedly between the species. A previous study in the mouse identified *Hox*a10 in the prostate anlage before birth but no expression thereafter (12). The postnatal increase in *Hox*a10 expression in the rat prostate is thus very dissimilar. In mouse prostate, Bushman *et al.* found that *Hox*a13 and *Hox*d13 expression levels decreased from birth to adulthood (4,5), whereas the opposite was observed here for rat prostate. The relative levels of the *Hox*13 genes in the separate prostate lobes also appear to differ between the mouse and rat. In the present study, *Hox*a13 and *Hox*d13 expression peaked in the rat DP with an anterior boundary at the epididymis. In contrast, murine expression levels for these genes peaked in the seminal vesicles, not in the prostate gland, and was present in the epididymis (4,11). Although a strict increasing anterior-to-posterior gradient in *Hox*b13 expression was observed in the adult rat prostate lobes (7), equivalent expression levels were found in the mouse VP and LP, whereas the DP and coagulating gland had 2- to 3-fold lower expression (7). Furthermore, *Hox*b13 expression was restricted to the VP during postnatal development in the murine prostate (9), whereas it was expressed at equivalent levels in the VP, DP, and LP at postnatal d 10 in the present study. We propose that these distinct differences in *Hox* gene expression levels and patterns between the two rodent species are critical factors in determining the morphological differences between their prostate lobes.

The present results determined that *Hox*b13 expression has a distinct anterior boundary in the male reproductive tract with expression found only in structures derived from the UGS. Because the coagulating gland (also referred to as the anterior prostate) is derived from mesodermal mesenchyme and UGS epithelium, a low but detectable level of *Hox*b13 expression was found in this structure. The strict increasing anterior-to-posterior expression gradient with the VP expressing the highest levels indicates that *Hox*b13 expression is essential not only for prostate gland identity in general, but for posterior lobe characteristics in particular. It is interesting to note that *HOX*b13 is highly expressed in the human prostate gland and based on the peak expression in the rodent VP, it has been suggested that the VP may bear a greater resemblance to the human prostate gland than previously attributed (18).

Previous studies with transgenic *Hox*b13 null mice indicated that this gene plays a critical role in epithelial cell differentiation because loss of secretory gene production and cell polarity were observed in the VP (9). Using an alternate approach with forced expression of *Hox*b13 in a rat prostate basal epithelial cell line, the present findings confirm a critical developmental role for *Hox*b13 in driving prostate epithelial cells into a differentiated luminal cell phenotype. Similar results were obtained with transfection of *Hox*b13 in PC3 and LNCaP human prostate cancer

cells where a shift toward a differentiated morphology was observed, suggesting a role for *Hox*b13 in maintenance of luminal cell differentiation in the adult prostate (13,16). Recent studies with epidermal cells (38) and kidney cells (39) also noted terminal differentiation after the introduction of the *Hox*b13 gene indicating that *Hox*b13 can promote differentiation in a variety of cells.

Androgens are essential and sufficient for prostate development and continued androgen levels are required throughout life for prostate gland homeostasis. In the present study, we observed that androgens increased the expression of all examined *Hox* genes in the developing rat VP, which suggests that androgenic regulation of these genes may specifically contribute to prostate morphogenesis. Interestingly, *Hox* gene expression was unaffected by androgens in the LP, which indicates a lobe-specific hormonal regulation of *Hox* genes. It has been previously shown that the LP is far less responsive to androgens than the VP (37,40–44), and androgen-independent expression of *Hox* genes may be a contributing factor for the relative androgen independence in that lobe. In contrast to the developing prostate gland, the current findings show that *Hox* gene expression in the adult rat prostate lobes was less affected by androgens. Furthermore, the few androgenic effects observed were gene and lobe specific. In the VP, androgens appear to down-regulate adult expression of *Hox*a9 and *Hox*a13 because their expression levels increase on androgen withdrawal. In contrast, these genes were unaffected by androgen ablation in the DP and LP. Furthermore, *Hox*b13 was significantly decreased in the DP and LP but only marginally affected by androgen removal in the VP, which suggests that androgens up-regulate *Hox*b13 in a region-specific manner in the rat prostate gland. Previous studies with the murine prostate did not observe androgenic effects on *Hox*b13 expression (7) and the present findings may reflect another specific difference in *Hox* gene expression.

In summary, we have identified unique *Hox* codes for the separate lobes of the rat prostate gland and the more anterior male reproductive tract organs and propose that this contributes to the organ-specific and prostate lobe-specific identity of these separate structures. Of particular importance, *Hox*b13 is specifically involved in prostate gland identity within the male reproductive tract structures where it plays a critical role in epithelial cell differentiation to a luminal phenotype. Androgens regulate prostatic *Hox* gene expression in a lobe-specific manner during development and in a gene-specific manner in the adult prostate gland. We conclude that the prostatic *Hox* genes reach a destined expression level at specific developmental time points and suggest that this timely *Hox* code participates in determining lobe-specific prostatic identity and cellular differentiation.

Acknowledgements

This work was supported by National Institutes of Health Grant DK40890 (G.S.P.) and American Foundation of Urologic Disease (L.H.).

Abbreviations

BOCM
: Basic organ culture medium

CK
: cytokeratin

DP
: dorsal prostate

LP
: lateral prostate

UGS

endodermal urogenital sinus

VP

ventral prostate

References

1. Gehring, W. The discovery of the homeobox. In: Duboule, D., editor. Guidebook to the homeobox genes. New York: Oxford University Press; 1994. p. 3-10.
2. Krumlauf R. *Hox* genes in vertebrate development. Cell 1994;78:191–201. [PubMed: 7913880]
3. Warot X, Fromental-Ramain C, Fraulob V, Chambon P, Dolle P. Gene dosage-dependent effects of the *Hox*a-13 and *Hox*d-13 mutations on morphogenesis of the terminal parts of the digestive and urogenital tracts. Development 1997;124:4781–4791. [PubMed: 9428414]
4. Podlasek CA, Clemens JQ, Bushman W. *Hox*a-13 gene mutation results in abnormal seminal vesicle and prostate development. J Urol 1999;161:1655–1661. [PubMed: 10210434]
5. Oefelein M, Chin-Chance C, Bushman W. Expression of the homeotic gene *Hox*-d13 in the developing and adult mouse prostate. J Urol 1996;155:342–346. [PubMed: 7490883]
6. Podlasek CA, Duboule D, Bushman W. Male accessory sex organ morphogenesis is altered by loss of function of *Hox*d-13. Dev Dyn 1997;208:454–465. [PubMed: 9097018]
7. Sreenath T, Orosz A, Fujita K, Bieberich CJ. Androgen-independent expression of *hox*b-13 in the mouse prostate. Prostate 1999;41:203–207. [PubMed: 10517879]
8. Prins GS, Birch L, Habermann H, Chang WY, Tebeau C, Putz O, Bieberich C. Influence of neonatal estrogens on rat prostate development. Reprod Fertil Dev 2001;13:241–252. [PubMed: 11800163]
9. Economides KD, Capecchi MR. *Hox*b13 is required for normal differentiation and secretory function of the ventral prostate. Development 2003;130:2061–2069. [PubMed: 12668621]
10. Takahashi Y, Hamada J, Murakawa K, Takada M, Tada M, Nogami I, Hayashi N, Nakamori S, Monden M, Miyamoto M, Katoh H, Moriuchi T. Expression profiles of 39 *HOX* genes in normal human adult organs and anaplastic thyroid cancer cell lines by quantitative real-time RT-PCR system. Exp Cell Res 2004;293:144–153. [PubMed: 14729064]
11. Liao X, Thrasher JB, Holzbeierlein J, Stanley S, Li B. Glycogen synthase kinase-3β activity is required for androgen-stimulated gene expression in prostate cancer. Endocrinology 2004;145:2941–2949. [PubMed: 14988390]
12. Podlasek CA, Seo RM, Clemens JQ, Ma L, Maas RL, Bushman W. *Hox*a-10 deficient male mice exhibit abnormal development of the accessory sex organs. Dev Dyn 1999;214:1–12. [PubMed: 9915571]
13. Jung C, Kim RS, Zhang H, Lee SJ, Jeng MH. *HOX*B13 induces growth suppression of prostate cancer cells as a repressor of hormone-activated androgen receptor signaling. Cancer Res 2004;64:9185–9192. [PubMed: 15604291]
14. Miller G, Miller HL, van Bokhoven A, Lambert J, Werahera P, Schirripa O, Luccia M, Nordeen S. Aberrant *HOX*C expression accompanies the malignant phenotype in prostate cancer. Cancer Res 2003;63:5879–5888. [PubMed: 14522913]
15. Hostikka S, Capecchi M. The mouse *Hox*c11 gene: genomic structure and expression pattern. Mech Dev 1998;70:133–145. [PubMed: 9510030]
16. Jung C, Kim RS, Lee SJ, Wang C, Jeng MH. *HOX*B13 homeodomain protein suppresses the growth of prostate cancer cells by the negative regulation of T-cell factor 4. Cancer Res 2004;64:3046–3051. [PubMed: 15126340]
17. Waltregny D, Alami Y, Clausse N, de Leval J, Castronovo V. Overexpression of the homeobox gene *HOX*C8 in human prostate cancer correlates with loss of tumor differentiation. Prostate 2002;50:162–169. [PubMed: 11813208]
18. Edwards S, Campbell C, Flohr P, Shipley J, Giddings I, Te-Poele R, Dodson A, Foster C, Clark J, Jhavar S, Kovacs G, Cooper CS. Expression analysis onto microarrays of randomly selected cDNA clones highlights *HOX*B13 as a marker of human prostate cancer. Br J Cancer 2005;92:376–381. [PubMed: 15583692]

19. Williams TM, Williams ME, Kuick R, Misek D, McDonagh K, Hanash S, Innis JW. Candidate downstream regulated genes of *HOX* group 13 transcription factors with and without monomeric DNA binding capability. Dev Biol 2005;279:462–480. [PubMed: 15733672]
20. Daftary GS, Taylor HS. Endocrine regulation of *HOX* genes. Endocr Rev 2006;27:331–355. [PubMed: 16632680]
21. Marshall H, Morrison A, Studer M, Popperl H, Krumlauf R. Retinoids and *hox* genes. FASEB J 1996;9:969–978. [PubMed: 8801179]
22. Ma L, Benson GV, Lim H, Dey SK, Maas RL. Abdominal B(AbdB) *hox*a genes: regulation in adult uterus by estrogen and progesterone and repression in mullerian duct by the synthetic estrogen diethylstilbestrol (DES). Dev Biol 1998;197:141–154. [PubMed: 9630742]
23. Lim H, Ma L, Ma W, Maas RL, Dey SK. Hoxa-10 regulates uterine stromal cell responsiveness to progesterone during implantation and decidualization in the mouse. Mol Endocrinol 1999;13:1005–1017. [PubMed: 10379898]
24. Price, D. Comparative aspects of development and structure in the prostate. In: Vollmer, EP., editor. Biology of the prostate and related tissues. 12. Washington, DC: National Cancer Institute; 1963. p. 1-27.
25. Lee C, Tsai Y, Harrison HH, Sensibar J. Proteins of the rat prostate: I. Preliminary characterization by two-dimensional electrophoresis. Prostate 1985;7:171–182. [PubMed: 4048014]
26. Matusik RJ, Kreis C, McNicol P, Sweetland R, Mullin C, Fleming WH, Dodd JG. Regulation of prostatic genes: role of androgens and zinc in gene expression. Biochem Cell Biol 1986;64:601–607. [PubMed: 3741677]
27. Hayashi N, Sugimura Y, Kawamura J, Donjacour AA, Cunha GR. Morphological and functional heterogeneity in the rat prostatic gland. Biol Reprod 1991;45:308–321. [PubMed: 1786296]
28. Stumpf, WE.; Sar, M. Autoradiographic localization of estrogen, androgen, progestin, and glucocorticosteroid in ‘target tissues’ and ‘nontarget tissues.’. In: Pasqualini, JR., editor. Receptors and Mechanisms of Action of Steroid Hormones. 8. New York: Marcel Dekker, Inc; 1976. p. 41-84.
29. Bomgardner D, Hinton BT, Turner TT. Hox transcription factors may play a role in regulating segmental function of the adult epididymis. J Androl 2001;22:527–531. [PubMed: 11451347]
30. Pu Y, Huang L, Prins GS. Sonic hedgehog-patched-gli signaling in the developing rat prostate gland: lobe-specific suppression by neonatal estrogens reduces ductal growth and branching. Dev Biol 2004;273:257–275. [PubMed: 15328011]
31. Danielpour D, Kadomatsu K, Anzano M, Smith J, Sporn M. Development and characterization of nontumorigenic and tumorigenic epithelial cell lines from rat dorsal-lateral prostate. Cancer Res 1994;54:3413–3421. [PubMed: 8012960]
32. Danielpour D. Transdifferentiation of NRP-152 rat prostatic basal epithelial cells toward a luminal phenotype: regulation by glucocorticoid, insulin-like growth factor-I and transforming growth factor-*β*. J Cell Sci 1999;112:169–179. [PubMed: 9858470]
33. Duan Y, Chen D, Chui C. Prostate-specific targeting using PSA promoter-based lentiviral vectors. Cancer Gene Therapy 2001;8:628–635. [PubMed: 11593331]
34. Huang L, Pu Y, Alam S, Birch L, Prins GS. The role of Fgf10 signaling in branching morphogenesis and gene expression in the rat prostate gland: lobe-specific suppression by neonatal estrogens. Dev Biol 2005;278:396–414. [PubMed: 15680359]
35. Hayward S, Haughney P, Lopes E, Danielpour D, Cunha G. The rat prostatic epithelial cell line NRP-152 can differentiate in vivo in response to its stromal environment. Prostate 1999;39:205–212. [PubMed: 10334110]
36. Sadan O, van Iddekinge B, Savage N, van der Walt L, Zakut H. Endocrine profile associated with estrogen and progesterone receptors in leiomyoma and normal myometrium. Gynecol Endocrinol 1990;4:33–42. [PubMed: 2110713]
37. Lee, C. The prostatic cell: structure and function. New York: Alan R. Liss; 1981. Physiology of castration-induced regression in rat prostate; p. 145-159.
38. Mack JA, Li LC, Sato N, Hascall VC, Maytin EV. *Hox*b13 up-regulates transglutaminase activity and drives terminal differentiation in an epidermal organotypic model. J Biol Chem 2005;280:29904–29911. [PubMed: 15964834]

39. Okuda H, Toyota M, Ishida W, Furihata M, Tsuchiya M, Kamada M, Tokino T, Shuin T. Epigenetic inactivation of the candidate tumor suppressor gene *HOX*B13 in human renal cell carcinoma. Oncogene 2006;25:1733–1742. [PubMed: 16278676]

40. Shain SA, Boesel RW. Aging-associated diminished rat prostate androgen receptor content concurrent with decreased androgen dependence. Mech Aging Dev 1977;6:219–232. [PubMed: 559225]

41. Witorsch RJ. Regional variations in the testicular dependence of prolactin binding and its possible relationship to castration-induced involution in rat prostate gland. Prostate 1982;3:459–473. [PubMed: 6292885]

42. Prins GS, Birch L, Greene GL. Androgen receptor localization in different cell types of the adult rat prostate. Endocrinology 1991;129:3187–3199. [PubMed: 1954898]

43. Prins GS. Differential regulation of androgen receptors in the separate rat prostate lobes: androgen independent expression in the lateral lobe. J Steroid Biochem 1989;33:319–326. [PubMed: 2779222]

44. Prins GS, Woodham C. Autologous regulation of androgen receptor mRNA in the separate lobes of the rat prostate gland. Biol Reprod 1995;53:609–619. [PubMed: 7578685]

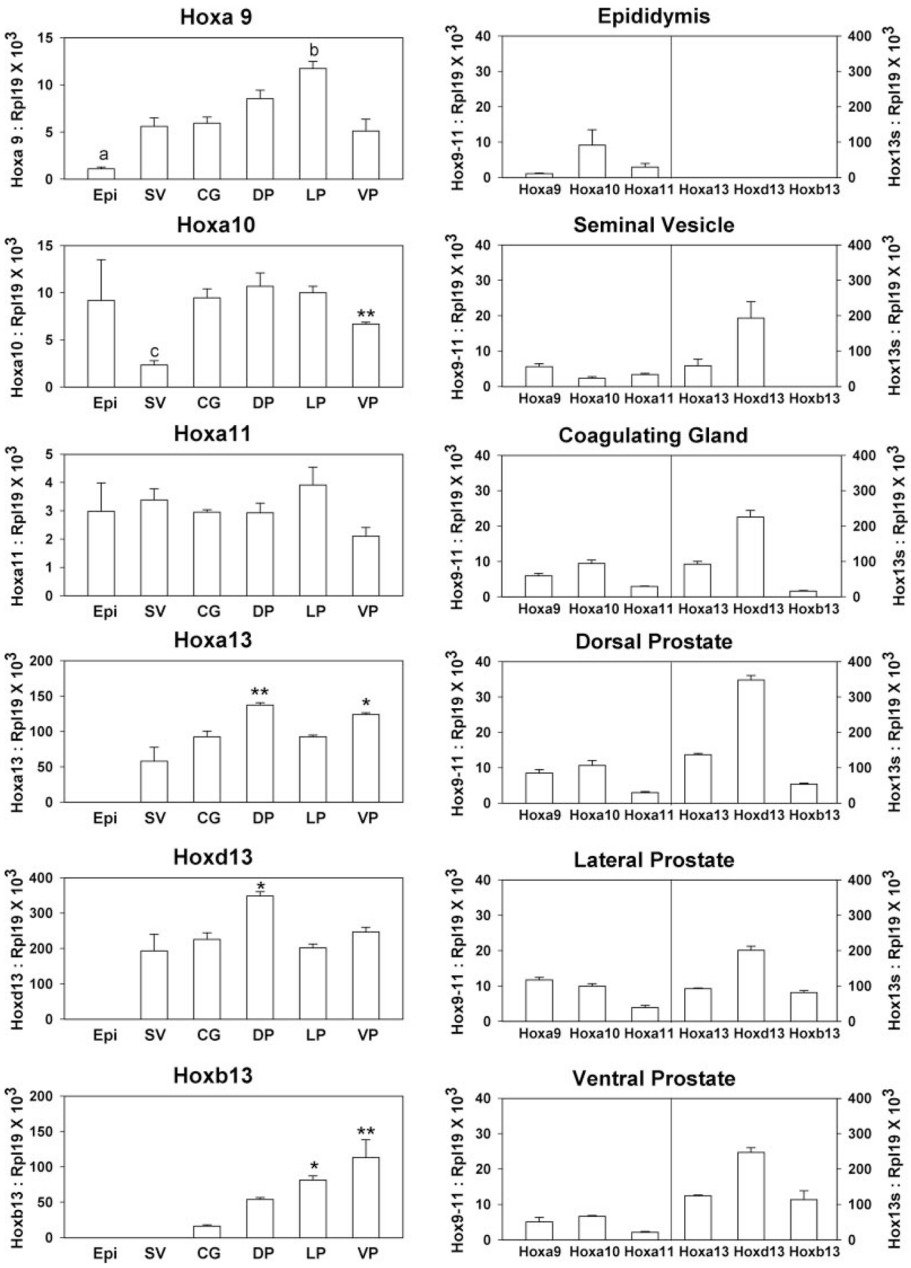

Fig. 1.

Quantitation of posterior *Hox* gene expression in the adult male accessory sex glands. Real-time RT-PCR was used to measure *Hox*a9, *Hox*a10, *Hox*a11, *Hox*a13, *Hox*d13, and *Hox*b13 mRNA levels in d 90 intact rat epididymis (Epi), seminal vesicle (SV), coagulating gland (CG), DP, LP, and VP. *Bars* represent mean ± SEM for three to 11 replicates. The *left column* shows expression levels for each individual *Hox* gene within the different structures along the anterior-to-posterior axis. *Hox*b13 is noted for the most striking colinear gradient along the anterior-to-posterior axis. Significance levels for each genes are: *Hox*a9, a, $P < 0.001$ *vs.* DP and LP; b, $P < 0.01$ *vs.* SV, CG, and VP; *Hox*a10, c, $P < 0.05$ *vs.* all groups, **, $P < 0.01$ *vs.* LP; *Hox*a11, no significant differences; *Hox*a13, *, $P < 0.05$; **, $P < 0.01$ *vs.* SV; *Hox*d13; *, $P < 0.05$ *vs.* SV and LP; *Hox*b13, *, $P < 0.05$; **, $P < 0.01$ *vs.* CG. The *right column* shows the posterior *Hox* code for each individual male accessory sex gland. The combination of *Hox* genes differs

among the various structures, constituting a unique *Hox* code for each tissue. Notably, the anterior boundary for all *Hox*13 genes is at the epididymis, which does not express any *Hox*13 paralog. Although *Hox*a13 and *Hox*d13 are expressed in the seminal vesicles, *Hox*b13 expression is restricted to UGS-derived structures. The most anterior of the prostate lobes, the DP, has the highest expression levels of *Hox*a13 and *Hox*d13 but low *Hox*b13 expression. The LP has the lowest expression of *Hox*a13 and *Hox*b13 and moderate *Hox*d13 levels. The posterior VP is distinct from the other two lobes with the highest expression of *Hox*b13 mRNA and the lowest levels of the anterior *Hox*a9, *Hox*a10, and *Hox*a11 genes.

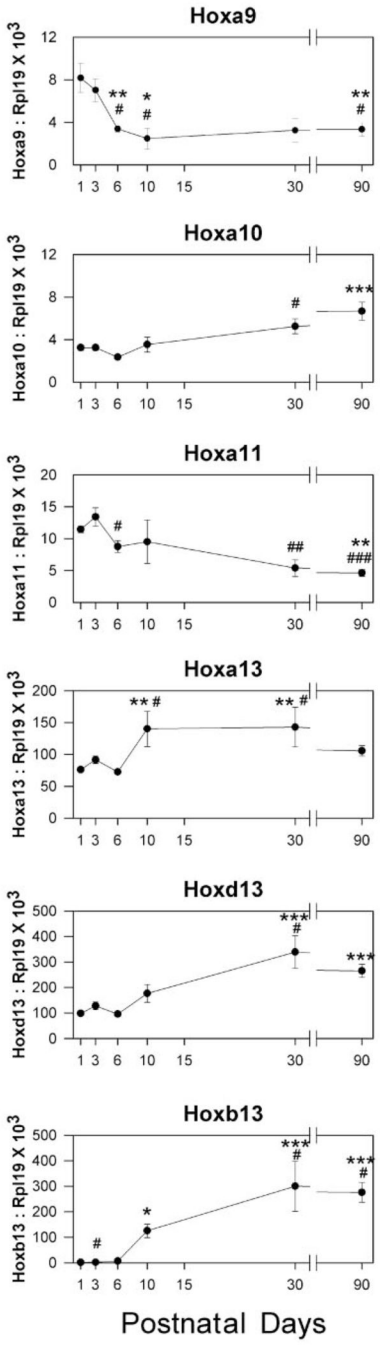

Fig. 2.

Ontogeny of *Hox*a9, *Hox*a10, *Hox*a11, *Hox*a13, *Hox*d13, and *Hox*b13 expression in the rat ventral prostate from birth through adulthood. *Hox*a9 expression is high at birth and decreases by d 6 to a constant lower level through adulthood. *, $P < 0.05$; **, $P < 0.01$ *vs.* d 1; #, $P < 0.05$ *vs.* d 3. *Hox*a10 levels are low at birth and gradually increase after d 10 to a 2-fold higher level in adulthood. ***, $P < 0.001$ *vs.* d 1, 3, and 6; #, $P < 0.05$ *vs.* d 6. *Hox*a11 expression is highest at d 3 and decreases thereafter to one third of this level by d 90. **, $P < 0.01$ *vs.* d 1; #, $P < 0.05$ *vs.* d 3; ##, $P < 0.01$ *vs.* d 3; ###, $P < 0.001$ *vs.* d 3. The *Hox*13 genes are expressed at 10-fold or greater levels compared with the anterior *Hox*a9–11 genes. The expression of all *Hox*13 genes are lowest during early prostate development and increase to the highest

expression levels in the adult VP. *Hox*a13 and *Hox*d13 increase 2- to 3-fold, whereas *Hox*b13 expression increases 200-fold by adulthood. *Hox*a13, ***, $P < 0.001$ *vs.* d 1 and 6, #, $P < 0.05$ *vs.* d 3; *Hox*d13, ***, $P < 0.001$ *vs.* d 1, 3 and 6, #, $P < 0.05$ *vs.* d 10; *Hox*b13, ***, $P < 0.001$ *vs.* d 1, 3, and 6, #, $P < 0.05$ *vs.* d 10. Each *point* represents the mean ± SEM for three to 11 replicates.

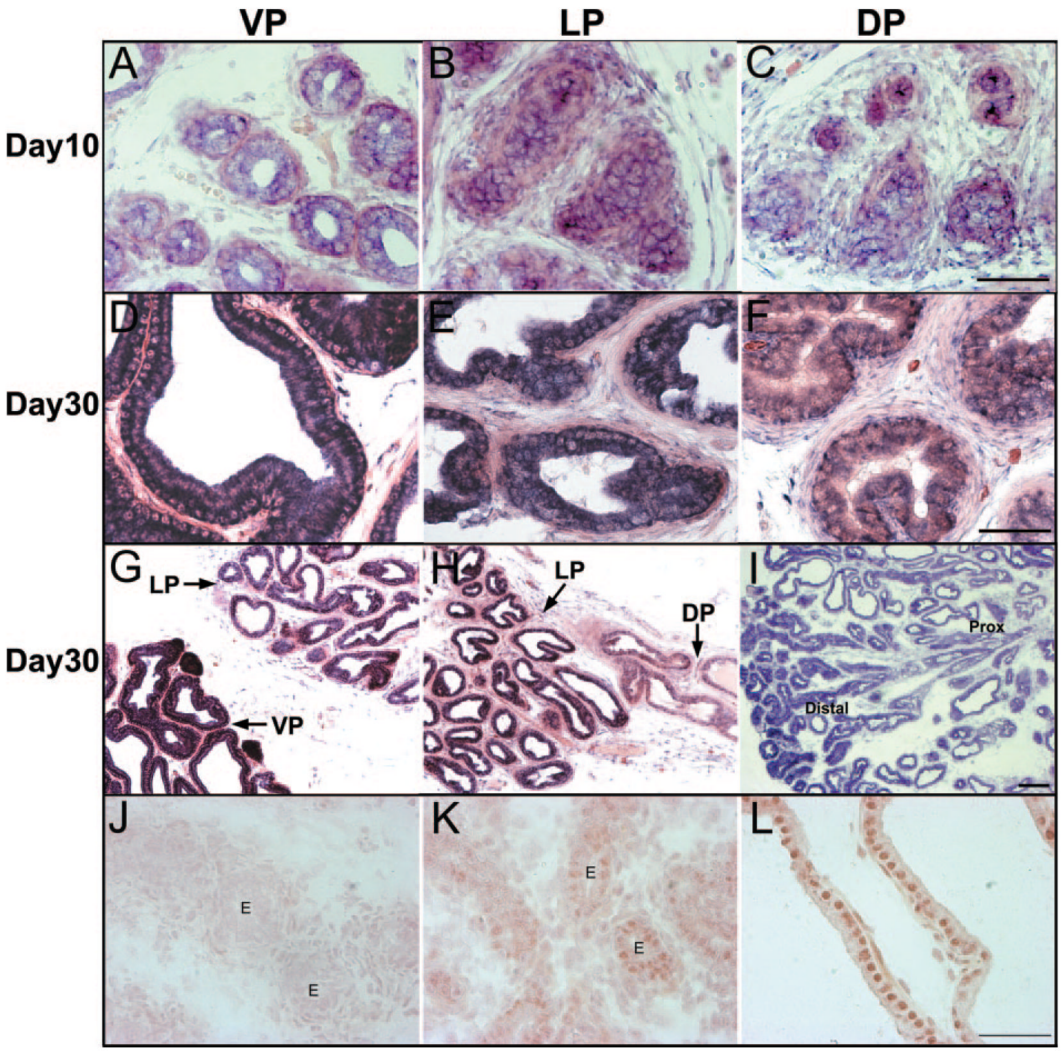

Fig. 3.

In situ hybridization (ISH) for *Hox*b13 expression (A–I) and immunohistochemistry (IHC) for *Hox*b13 protein localization (J–L) in the developing rat prostate. For ISH, sections from d 10 and 30 intact prostates were processed together to allow direct comparisons of signal strength. For IHC, intact prostate sections from d 6, 10, and 30 were processed together to allow direct comparisons of stain intensity. At d 10, *Hox*b13 mRNA signal was similar among the (A) VP, (B) LP, and (C) DP lobes. By d 30, a distinct expression gradient was observed with (D) highest expression in the VP, (E) moderate expression in the LP, and (F) lowest expression levels in the DP. This gradient is best observed at (G and H) lower power of a whole prostatic complex on a single slide where the adjacent lobes can be directly compared. A longitudinal gradient along the ductal length was also apparent with intense *Hox*b13 expression in the distal regions of all lobes and low signal intensity in the proximal ducts (I). IHC staining of *Hox*b13 protein in the VP on d (J) 6, (K) 10, and (L) 30 revealed low protein staining in epithelial nuclei and strong *Hox*b13 protein levels by d 30 (E, epithelial ducts; *scale bar*, 50 μ_M).

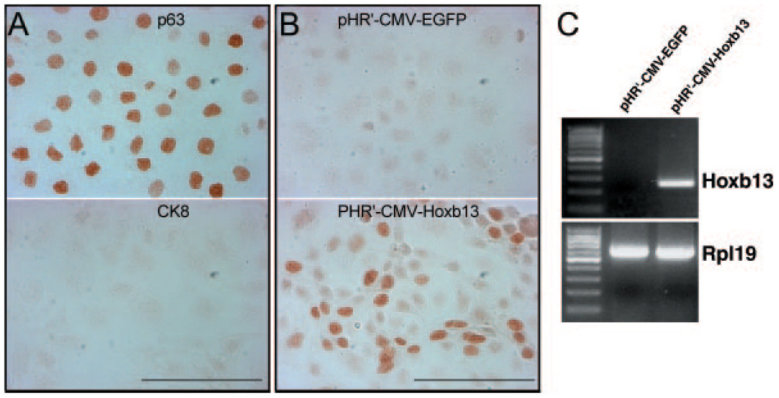

Fig. 4.

Differentiation status on *Hox*b13 expression in NRP-152 cells. A, NRP-152 cells grown in GM2 medium with 5% serum. Immunocytochemistry (ICC) staining of p63 (*top*) and CK8 (*bottom*) reveal a basal cell phenotype and absence of luminal cells under nondifferentiating growth condition. B, ICC of *Hox*b13 protein in lentiviral infected NRP-152 cells. No *Hox*b13 protein was found in pHR3-CMV-EGFP virus-infected cells (*top*). In NRP-152 cells infected with pHR3-CMV-*Hox*b13 virus, *Hox*b13 protein was localized to nuclei of infected cells (*bottom*). C, RT-PCR analysis of mRNA from lentiviral-infected NRP-152 cells. *Hox*b13 mRNA was not expressed in pHR3-CMV-EGFP virus-infected NRP-152 cells, whereas *Hox*b13 mRNA was expressed at high levels in pHR3-CMV-*Hox*b13 virus-infected cells (*scale bar*, 100 μ_M).

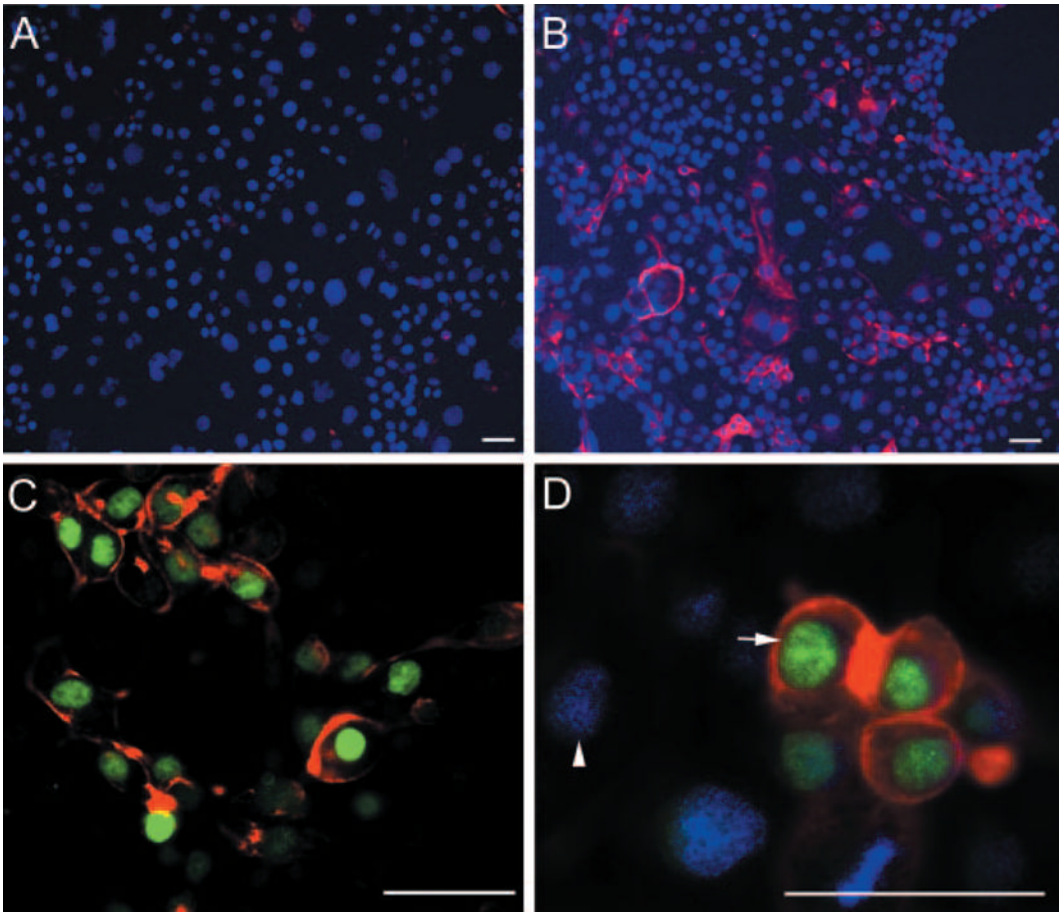

Fig. 5.

Forced expression of *Hox*b13 promotes differentiation of NRP152 cells. A, NRP-152 cells infected with pHR′-CMV-EGFP control vector immunostained with CK8 show lack of luminal cell differentiation. B, Cell culture infected with pHR′-CMV-*Hox*b13 showed robust CK8 staining in many cells after 72 h suggesting differentiation to a luminal phenotype. C and D, Colocalization of *Hox*b13 and CK8 in the same cells. C, All *Hox*b13 (*green*)-positive cells immunostained for CK8 (*red*) in the cytoplasm. D, Merged image of DAPI (*blue*)-stained cells reveals that *Hox*b13-negative nuclei (*arrowhead*) do not express CK8, whereas *Hox*b13 positive (*arrow*, *green*) cells express CK8 (*red*) (*scale bar*, 50 μM).

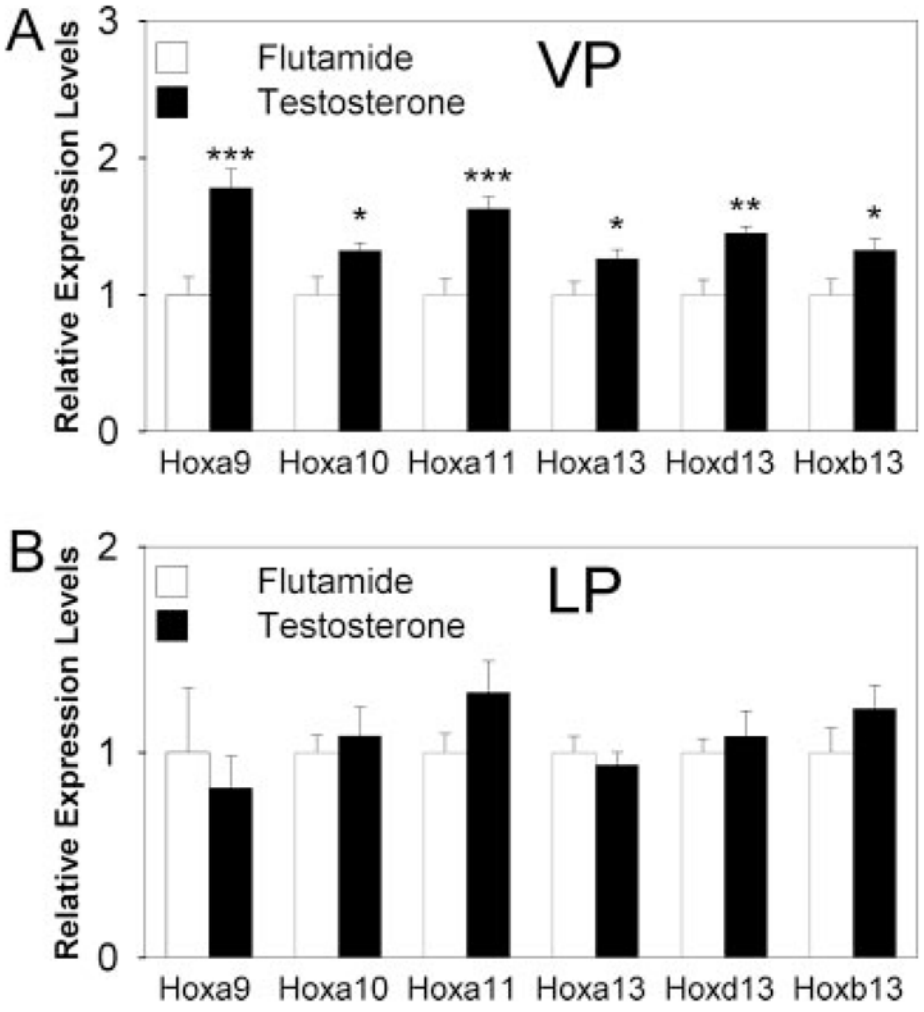

Fig. 6.

Androgen regulation of *Hox* gene expression in the developing VP and LP lobes. Contralateral VP and LP lobes from d 0 rats were cultured with 10 μ_M OH-flutamide (*open bar*) or 10 nM testosterone (*solid bar*) for 18 h. *Bars* represent mean ± SEM for 10 samples per treatment. A, All of the posterior *Hox* genes were up-regulated by testosterone in VP. *, $P < 0.05$; **, $P < 0.01$; ***, $P < 0.001$ testosterone *vs.* OH-flutamide treatment. B, LP *Hox* gene expression was not affected by the presence or absence of androgen action.

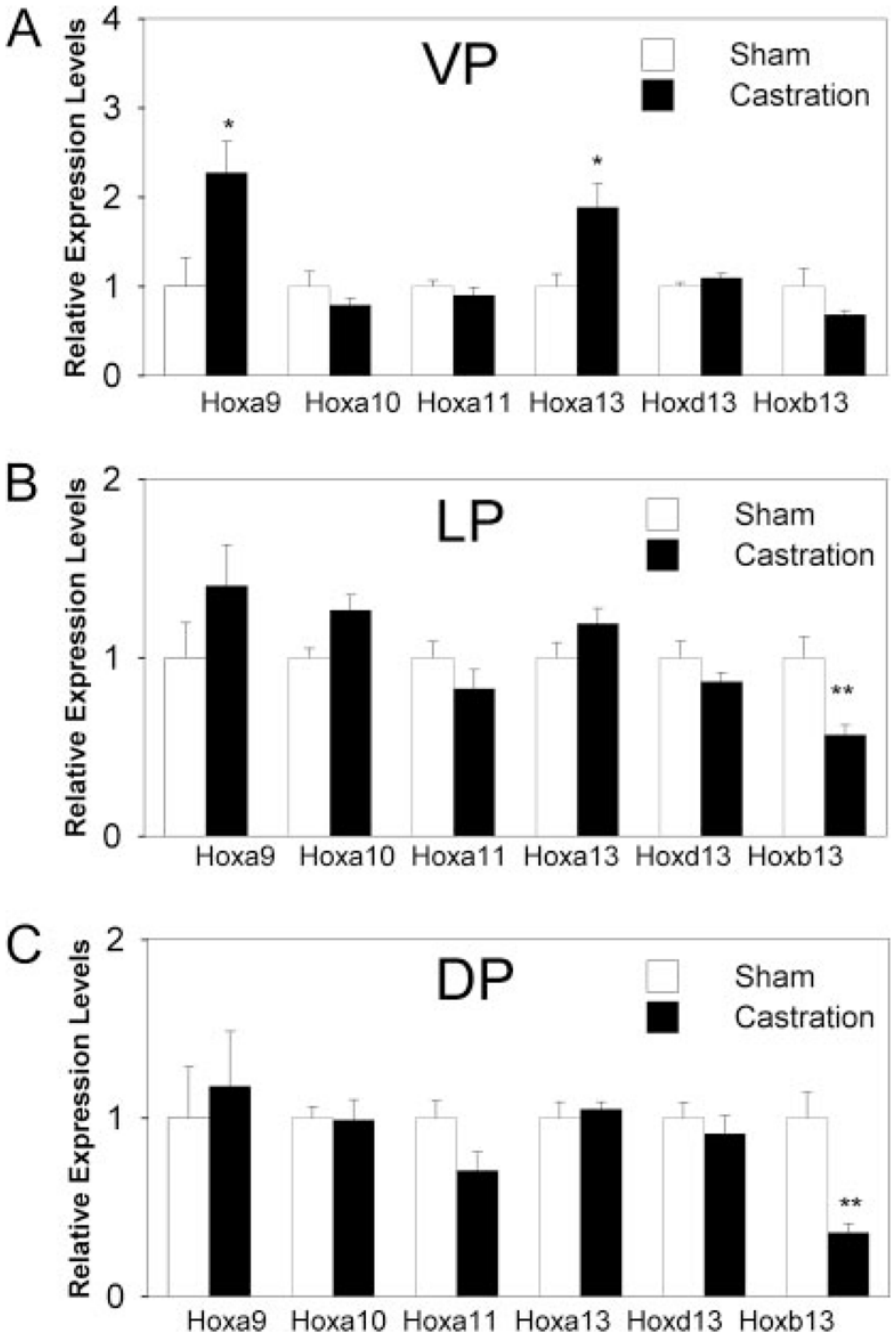

Fig. 7.

Effect of castration on *Hox* gene expression in the separate adult prostate lobes. Prostatic *Hox* gene expression was measured 48 h after castration and in sham-intact rats as controls. *Bars* represent mean ± SEM for six samples per treatment. A, Although expression of *Hox*a9 and *Hox*a13 was increased by androgen withdrawal in the adult VP, all other *Hox* genes were unaffected. B and C, *Hox* gene expression in the LP and DP, respectively, was largely unaffected by androgen withdrawal with the exception of *Hox*b13, which was significantly reduced. *, $P < 0.05$; **, $P < 0.01$ castration *vs.* sham.

TABLE 1

Primers and Taqman probes used for real-time PCR

Gene	Sequence	Amplicon size (bp)
*Hoxa*9		
Forward primer	aggaagagtaccgaggcaag	159
Reverse primer	taaatcactccgcacgctat	
Probe	ctgcgcgatccctttgcataaa	
*Hoxa*10		
Forward primer	aggactccctgggcaattc	83
Reverse primer	gtaagggcagcgtttcttcc	
*Hoxa*11		
Forward primer	gatctgcacccaaacctgag	159
Reverse primer	caaccagcaaaacctctgga	
Probe	ttctacctcccaatggtggtgatgg	
*Hoxa*13		
Forward primer	ctccccacctctggaagtc	139
Reverse primer	ttcgtagcgtattcccgttc	
*Hoxb*13		
Forward primer	gatgtgctgccaaggtgaac	83
Reverse primer	gaggagggtgctggacac	
Probe	aaagcagcgtttgcagagcc	
*Hoxd*13		
Forward primer	tagccaacgggtggaaca	125
Reverse primer	ccgacggtagacgcacat	
Probe	tgtattgtgccaaggaccagccg	
*Rpl*19		
Forward primer	ggaagcctgtgactgtccat	101
Reverse primer	ggcagtacccttcctcttcc	
Probe	aagggcaggcatatgggcat	